PHYSICAL REVIEW D **72,** 074015 (2005)

Analyticity properties of three-point functions in QCD beyond leading order

A. P. Bakulev*

Bogoliubov Laboratory of Theoretical Physics, JINR, 141980 Dubna, Russia

A. I. Karanikas†

University of Athens, Department of Physics, Nuclear and Particle Physics Section, Panepistimiopolis, GR-15771 Athens, Greece

N. G. Stefanis‡

Institut für Theoretische Physik II, Ruhr-Universität Bochum, D-44780 Bochum, Germany

(Received 9 May 2005; published 13 October 2005)

The removal of unphysical singularities in the perturbatively calculable part of the pion form factor—a classic example of a three-point function in QCD—is discussed. Different analytization procedures in the sense of Shirkov and Solovtsov are examined in comparison with standard QCD perturbation theory. We show that demanding the analyticity of the partonic amplitude as a *whole*, as proposed before by Karanikas and Stefanis, one can make infrared finite not only the strong running coupling and its powers, but also cure potentially large logarithms (that first appear at next-to-leading order) containing the factorization scale and modifying the discontinuity across the cut along the negative real axis. The scheme used here generalizes the analytic perturbation theory of Shirkov and Solovtsov to noninteger powers of the strong coupling and diminishes the dependence of QCD hadronic quantities on all perturbative scheme and scale-setting parameters, including the factorization scale.

DOI: 10.1103/PhysRevD.72.074015 PACS numbers: 12.38.Bx, 12.38.Lg, 13.40.Gp

I. INTRODUCTION

The phenomenology of QCD exclusive processes depends in a crucial way on the analytic properties of hadronic (hard) scattering amplitudes as functions of the strong running coupling. A perturbatively calculable short-distance part of the reaction amplitude at the parton level is isolated either by subtraction or by factorization. To get a quantitative interpretation of such quantities in practice and compare them with experimental data, one has to get rid of the artificial Landau singularity at $Q^2 = \Lambda_{\rm QCD}^2$ ($\Lambda_{\rm QCD} \equiv \Lambda$ in the following), where Q^2 is the large mass scale in the process. A proposal to solve this problem (in the spacelike region) without introducing exogenous infrared (IR) regulators, like an effective, or a dynamically generated, gluon mass [1] (see, for instance, [2–10] for such applications), was made by Shirkov and Solovtsov (SS) [11–13], based on general principles of local quantum field theory. This theoretical framework—termed analytic perturbation theory (APT)—was further expanded beyond the one-loop level of two-point functions to define an analytic[1] coupling and its powers in the timelike region [14–21], embracing previous attempts [22–27] in this direction.[2]

However, first applications [30,31] of this sort of approach to three-point functions, beyond the leading order of QCD perturbation theory, have made it clear that, ultimately, there must be an extension of this formalism from the level of the running coupling and its powers to the level of amplitudes. The reason is that in three-point functions at the next-to-leading order (NLO) level, and beyond, logarithms of a distinct scale (serving as the factorization or evolution scale) appear that though they do not change the nature of the Landau pole, they affect the discontinuity across the cut along the negative real axis $-\infty < Q^2 < 0$. On account of factorization, we expect that this effect should be small, of the order of a few percent, because any change caused by the variation of the factorization scale should be of the next higher order. However, to achieve a high-precision theoretical prediction, one should reduce this uncertainty, lifting the limitations imposed by the lack of knowledge about uncalculated higher-order corrections. To encompass such logarithmic terms in the "analytization" procedure, one should demand the analyticity of the partonic amplitude as a *whole* [32,33] and calculate the dispersive image of the coupling (or of its powers) *in conjunction* with these logarithms. This Karanikas–Stefanis (KS) analytization scheme effectively amounts to the generalization of APT to noninteger powers of the running coupling: fractional APT (FAPT), as we shall show below.

In this work we expand the Shirkov–Solovtsov analytization approach to include the dispersive images of such terms, using as a case study the pion form factor at NLO in the $\overline{\rm MS}$ scheme with various renormalization-scale settings and also in the α_V scheme [34]. To this end, we contrast the

*Electronic address: bakulev@theor.jinr.ru
†Electronic address: akaranik@cc.uoa.gr
‡Electronic address: stefanis@tp2.ruhr-uni-bochum.de

[1]The term "analyticity" is used here as a synonym for "spectrality" and "causality" [12].

[2]A somewhat different approach was reviewed recently in [28]; see also [29].

KS analytization with the *naive* [30,31] and the *maximal* [35] analytization procedures and work out their key mutual differences as they first appear in NLO, while a fully fledged analysis of FAPT is given in an accompanying paper [36]. We argue that augmenting the $\overline{\rm MS}$ scheme with the KS analytization prescription provides an optimized method to calculate perturbatively higher-order corrections to partonic "observables" in QCD because it practically eliminates all scheme and scale-setting ambiguities owing to the renormalization and factorization scales. It is worth emphasizing at this point that the focus of Ref. [32] was on the calculation of power corrections to the pion's electromagnetic form factor. Such contributions are outside the scope of the present investigation.

The plan of this paper is as follows. In Sec. II we review the convolution formalism for the calculation of the short-distance part of the pion form factor within perturbative QCD at NLO. In Sec. III we discuss the Shirkov-Solovtsov type analytization procedures [11,30–33,35] and work out their mutual differences, focusing on the KS analytization and its properties. This discussion extends and generalizes the original KS analysis that covered only the LO of the perturbative expansion of the pion form factor and ignoring evolution. Section 4 contains the results for the factorized pion form factor in different schemes and with different scale settings, employing the KS analytization in comparison with those based on APT and also standard QCD perturbation theory in NLO. Our conclusions with a summary of our main results are presented in Sec. V. Some important technical details are collected in three appendixes.

II. FACTORIZABLE PART OF THE PION FORM FACTOR AT NLO IN STANDARD QCD PERTURBATION THEORY

The leading-twist factorizable part of the electromagnetic pion form factor can be expressed as a convolution in the form [37,38]

$$F_{\pi}^{\rm Fact}(Q^2;\mu_{\rm R}^2) = \Phi_{\pi}^{*}(x,\mu_{\rm F}^2)\otimes_x T_{\rm H}(x,y,Q^2;\mu_{\rm F}^2,\mu_{\rm R}^2) \times \otimes_y \Phi_{\pi}(y,\mu_{\rm F}^2), \tag{2.1}$$

where $\otimes$ denotes the usual convolution symbol ($A(z)\underset{z}{\otimes} B(z)\equiv\int_0^1 dz A(z)B(z)$) over the longitudinal momentum fraction variable x (y) and $\mu_{\rm F}$ represents the factorization scale at which the separation between the long- (small transverse momentum) and short-distance (large transverse momentum) dynamics takes place, with $\mu_{\rm R}$ labelling the renormalization (coupling constant) scale. The nonperturbative input is encoded in the pion distribution amplitude (DA) $\Phi_{\pi}(y,\mu_{\rm F}^2)$, whereas the short-distance interactions are represented by the hard-scattering amplitude $T_{\rm H}(x,y,Q^2;\mu_{\rm F}^2,\mu_{\rm R}^2)$. This is the amplitude for a collinear valence quark-antiquark pair with total momentum P struck by a virtual photon with momentum q, satisfying $q^2=-Q^2$, to end up again in a configuration of a parallel valence quark-antiquark pair with momentum $P'=P+q$. It can be calculated perturbatively in the form of a power-series expansion in the QCD coupling, the latter to be evaluated at the reference scale of renormalization $\mu_{\rm R}^2$:

$$T_{\rm H}^{\rm NLO}(x,y,Q^2;\mu_{\rm F}^2,\mu_{\rm R}^2) = \alpha_s(\mu_{\rm R}^2)T_{\rm H}^{(0)}(x,y,Q^2) + \frac{\alpha_s^2(\mu_{\rm R}^2)}{4\pi}T_{\rm H}^{(1)}(x,y,Q^2;\mu_{\rm F}^2,\mu_{\rm R}^2). \tag{2.2}$$

The leading-order (LO) contribution to $T_{\rm H}(x,y,Q^2;\mu_{\rm F}^2)$ reads

$$T_{\rm H}^{(0)}(x,y,Q^2) = \frac{N_{\rm T}}{Q^2}\frac{1}{\bar{x}\,\bar{y}} \equiv \frac{1}{Q^2}t_{\rm H}^{(0)}(x,y), \tag{2.3}$$

where

$$N_{\rm T} = \frac{2\pi C_{\rm F}}{C_{\rm A}} = \frac{8\pi}{9}, \tag{2.4}$$

$C_{\rm F}=(N_{\rm c}^2-1)/2N_{\rm c}=4/3$, $C_{\rm A}=N_{\rm c}=3$ are the color factors of $SU(3)_{\rm c}$, and the notation $\bar{z}\equiv 1-z$ has been used. The usual color decomposition of the NLO correction [39]—marked by self-explainable labels—is given by (omitting the variables x and y)

$$Q^2T_{\rm H}^{(1)}(Q^2;\mu_{\rm F}^2,\mu_{\rm R}^2) = C_{\rm F}t_{\rm H}^{(1,{\rm F})}\left(\frac{\mu_{\rm F}^2}{Q^2}\right) + b_0 t_{\rm H}^{(1,\beta)}\left(\frac{\mu_{\rm R}^2}{Q^2}\right) + C_{\rm G}t_{\rm H}^{(1,{\rm G})}, \tag{2.5}$$

where $C_{\rm G}=(C_{\rm F}-C_{\rm A}/2)$ and b_0 is the first coefficient of the β function, see Appendix A, Eq. (A1). Here we explicitly factorized out a trivial $1/Q^2$ dependence and used for the coefficients in front of each factor the notation $t_{\rm H}$ with appropriate superscripts.

With reference to the application of the Brodsky-Lepage-Mackenzie (BLM) [40] scale setting in fixing the renormalization point later on, we single out the b_0-proportional (i.e., the N_f-dependent) term, given by

$$t_{\rm H}^{(1,\beta)}\left(x,y;\frac{\mu_{\rm R}^2}{Q^2}\right) = t_{\rm H,1}^{(1,\beta)}(x,y) + t_{\rm H,2}^{(1,\beta)}\left(x,y;\frac{\mu_{\rm R}^2}{Q^2}\right), \tag{2.6a}$$

with

$$t_{\rm H,1}^{(1,\beta)}(x,y) = t_{\rm H}^{(0)}(x,y)\left[\frac{5}{3}-\ln(\bar{x}\,\bar{y})\right], \tag{2.6b}$$

$$t_{\rm H,2}^{(1,\beta)}\left(x,y;\frac{\mu_{\rm R}^2}{Q^2}\right) = t_{\rm H}^{(0)}(x,y)\ln\frac{\mu_{\rm R}^2}{Q^2}, \tag{2.6c}$$

and present the color singlet part of $t_{\rm H}$ in the form

$$t_{\rm H}^{(1,{\rm F})}\left(x,y;\frac{\mu_{\rm F}^2}{Q^2}\right) = t_{\rm H,1}^{(1,{\rm F})}(x,y) + t_{\rm H,2}^{(1,{\rm F})}\left(x,y;\frac{\mu_{\rm F}^2}{Q^2}\right); \tag{2.7a}$$

$$t_{\rm H,2}^{(1,{\rm F})}\left(x,y;\frac{\mu_{\rm F}^2}{Q^2}\right) = t_{\rm H}^{(0)}(x,y)\left[2(3+\ln(\bar{x}\,\bar{y}))\ln\frac{Q^2}{\mu_{\rm F}^2}\right]. \tag{2.7b}$$

Explicit expressions for $t_{\mathrm{H},1}^{(1,\mathrm{F})}(x,y)$ and for the color nonsinglet part, $t_{\mathrm{H}}^{(1,\mathrm{G})}(x,y)$, cf. Eq. (2.5), are supplied in Appendix B [see Eqs. (B1) and (B2)].

The scaled hard-scattering amplitude, Eq. (2.2), truncated at the NLO and evaluated at the renormalization scale $\mu_{\mathrm{R}}^2 = \lambda_{\mathrm{R}} Q^2$, reads

$$Q^2 T_{\mathrm{H}}^{\mathrm{NLO}}(x,y,Q^2;\mu_{\mathrm{F}}^2,\lambda_{\mathrm{R}}Q^2) = \alpha_s(\lambda_{\mathrm{R}}Q^2) t_{\mathrm{H}}^{(0)}(x,y) + \frac{\alpha_s^2(\lambda_{\mathrm{R}}Q^2)}{4\pi} C_{\mathrm{F}} t_{\mathrm{H},2}^{(1,\mathrm{F})}\left(x,y;\frac{\mu_{\mathrm{F}}^2}{Q^2}\right) + \frac{\alpha_s^2(\lambda_{\mathrm{R}}Q^2)}{4\pi}\{b_0 t_{\mathrm{H}}^{(1,\beta)}(x,y;\lambda_{\mathrm{R}}) + t_{\mathrm{H}}^{(\mathrm{FG})}(x,y)\}, \tag{2.8}$$

where we have introduced the shorthand notation

$$t_{\mathrm{H}}^{(\mathrm{FG})}(x,y) \equiv C_{\mathrm{F}} t_{\mathrm{H},1}^{(1,\mathrm{F})}(x,y) + C_{\mathrm{G}} t_{\mathrm{H}}^{(1,\mathrm{G})}(x,y). \tag{2.9}$$

To calculate the factorizable part of the pion form factor, one has to convolute this expression with the pion DA for each hadron in the initial and final state. In leading-twist 2, the pion DA at the normalization scale $\mu_0^2 \approx 1\ \mathrm{GeV}^2$ is given by

$$\varphi_\pi(x,\mu_0^2) = 6x(1-x)[1 + a_2(\mu_0^2)C_2^{3/2}(2x-1) + a_4(\mu_0^2)C_4^{3/2}(2x-1) + \ldots], \tag{2.10}$$

with all nonperturbative information being encapsulated in the Gegenbauer coefficients a_n. In this analysis we use those coefficients determined before by Bakulev, Mikhailov, and Stefanis (BMS) in [41] with the aid of QCD sum rules with nonlocal condensates:

$$a_2^{\mathrm{BMS}} = 0.20, \qquad a_4^{\mathrm{BMS}} = -0.14, \qquad a_n^{\mathrm{BMS}} = 0, n > 4, \tag{2.11}$$

where the vacuum quark virtuality $\lambda_q^2 = 0.4\ \mathrm{GeV}^2$ has been used. This set of values was found [42,43] to be consistent at the 1σ level with the high-precision CLEO data [44] on the pion-photon transition form factor, with all other model DAs being outside—at least—the 2σ error ellipse (see [45] for the latest compilation of models in comparison with the CLEO and CELLO [46] data). Notice that the particular parametrization (shape) of the pion DA chosen is irrelevant for the considerations to follow.

III. ANALYTICITY OF PARTONIC AMPLITUDES BEYOND LO

A. Analytic running coupling in QCD

The main stumbling block in applying fixed-order perturbation theory at low momenta Q^2 is the nonphysical Landau singularity of the running strong coupling at $Q^2 = \Lambda^2$, which entails the appearance of IR renormalons in the perturbative expansion. To ensure the analyticity of the coupling in the infrared, one can follow different strategies [11,25,27,47–51] all based on the basic assumption that the *physical* coupling should stay IR finite and analytic in the whole momentum range, though its precise value at $Q^2 = 0$ is still a matter of debate [11,21,28,52,53]. Imposing the analyticity of the coupling in the sense of Shirkov and Solovtsov [11], we replace the strong running coupling and its powers by their analytic versions:

$$[\alpha_s^{(n)}(Q^2)^m]^{\mathrm{an}} \equiv \mathcal{A}_m^{(n)}(Q^2) \quad \text{with} \quad [f(Q^2)]^{\mathrm{an}} = \frac{1}{\pi}\int_0^\infty \frac{\mathbf{Im}[f(-\sigma)]}{\sigma + Q^2 - i\epsilon} d\sigma, \tag{3.1}$$

where the loop order is explicitly indicated by the superscript n in parenthesis and

$$\mathcal{A}_1^{(1)}(Q^2) = \frac{4\pi}{b_0}\left[\frac{1}{\ln(Q^2/\Lambda^2)} + \frac{\Lambda^2}{\Lambda^2 - Q^2}\right] \equiv \bar{\alpha}_s(Q^2), \tag{3.2}$$

with the last step connecting to the SS notation [11], and $\alpha_s(0) = 4\pi/b_0$. The two-loop running coupling in standard QCD perturbation theory can be expressed [19] in terms of the Lambert function W_{-1} to read

$$\alpha_s^{(2)}(Q^2) = -\frac{4\pi}{b_0 c_1}\left[1 + W_{-1}\left(-\frac{1}{c_1 e}\left(\frac{\Lambda^2}{Q^2}\right)^{1/c_1}\right)\right]^{-1}. \tag{3.3}$$

For some more explanations we refer the interested reader to [42], Appendix C, Eqs. (C15) and (C20). Then, the analytic image of the kth power of the coupling [14] is obtained from the dispersion relation

$$\mathcal{A}_k^{(2)}(Q^2) = \frac{1}{\pi}\int_0^\infty d\sigma \frac{\rho_k^{(2)}(\sigma)}{\sigma + Q^2 - i\epsilon} \tag{3.4}$$

with the spectral density

$$\rho_k^{(2)}(t) = \left(\frac{4\pi}{b_0 c_1}\right)^k \mathbf{Im}\left(-\frac{1}{1 + W_1(z(t))}\right)^k. \tag{3.5}$$

In the numerical calculations below, we use an approximate form suggested in [35]:

$$\mathcal{A}_1^{(2,\mathrm{fit})}(Q^2) = \frac{4\pi}{b_0}\left\{\frac{1}{\ell[\ln(Q^2/\Lambda_{21}^2), c_{21}^{\mathrm{fit}}]} + \frac{1}{1 - \exp(\ell[\ln(Q^2/\Lambda_{21}^2), c_{21}^{\mathrm{fit}}])}\right\}; \tag{3.6}$$

$$\mathcal{A}_2^{(2,\mathrm{fit})}(Q^2) = \left(\frac{4\pi}{b_0}\right)^2\left\{\frac{1}{\ell[\ln(Q^2/\Lambda_{22}^2), c_{22}^{\mathrm{fit}}]^2} - \frac{\exp(\ell[\ln(Q^2/\Lambda_{22}^2), c_{22}^{\mathrm{fit}}])}{[1 - \exp(\ell[\ln(Q^2/\Lambda_{22}^2), c_{22}^{\mathrm{fit}}])]^2}\right\}, \tag{3.7}$$

where the values of the fit parameters are listed in Table I

TABLE I. Parameters entering Eqs. (3.6) and (3.7) for the value $\Lambda_{\rm QCD}^{N_f=3} = 400$ MeV.

Parameters	$c_{21}^{\rm fit}$	Λ_{21}	$c_{22}^{\rm fit}$	Λ_{22}
Values	-1.015	67 MeV	-1.544	34.5 MeV

and

$$\ell[L, c] \equiv L + c \ln\sqrt{L^2 + 4\pi^2}. \tag{3.8}$$

B. Analytization procedures

Let us now see how analyticity can be implemented on the parton-level pion form factor in NLO accuracy of perturbative QCD. We discuss three analytization procedures[3]:

(i) *Naive* analytization [30,31,35]

$$[Q^2 T_{\rm H}(x, y, Q^2; \mu_{\rm F}^2, \lambda_{\rm R} Q^2)]_{\rm SS}^{\rm naive\text{-}an} = \mathcal{A}_1^{(2)}(\lambda_{\rm R} Q^2) t_{\rm H}^{(0)}(x, y) + \frac{(\mathcal{A}_1^{(2)}(\lambda_{\rm R} Q^2))^2}{4\pi} \times \left[b_0 t_{\rm H}^{(1,\beta)}(x, y; \lambda_{\rm R}) + t_{\rm H}^{(\rm FG)}(x, y) + C_{\rm F} t_{\rm H,2}^{(1,\rm F)}\left(x, y; \frac{\mu_{\rm F}^2}{Q^2}\right)\right]. \tag{3.9}$$

(ii) *Maximal* analytization [35]

$$[Q^2 T_{\rm H}(x, y, Q^2; \mu_{\rm F}^2, \lambda_{\rm R} Q^2)]_{\rm SS}^{\rm max\text{-}an} = \mathcal{A}_1^{(2)}(\lambda_{\rm R} Q^2) t_{\rm H}^{(0)}(x, y) + \frac{\mathcal{A}_2^{(2)}(\lambda_{\rm R} Q^2)}{4\pi} \times \left[b_0 t_{\rm H}^{(1,\beta)}(x, y; \lambda_{\rm R}) + t_{\rm H}^{(\rm FG)}(x, y) + C_{\rm F} t_{\rm H,2}^{(1,\rm F)}\left(x, y; \frac{\mu_{\rm F}^2}{Q^2}\right)\right]. \tag{3.10}$$

(iii) *Amplitude* analytization proposed by Karanikas and Stefanis in [32,33].

The first method replaces α_s and its powers by the Shirkov-Solovtsov analytic coupling [11] and its powers, whereas the second one uses for the powers of α_s their own analytic images, transforming this way the power-series expansion in $[\alpha_s(Q^2)]^n$ in a functional expansion in terms of the functions $\mathcal{A}_n(Q^2)$ [13,16]. Imposing analyticity in the sense of Karanikas-Stefanis [32], differs from the previous two approaches in that it demands the *whole* partonic amplitude has the correct analytical behavior as a function of Q^2. This entails the analytization of terms of the form $(\alpha_s^{(n)}(Q^2))^m \ln(Q^2/\mu_{\rm F}^2)$, which appear in exclusive amplitudes at NLO of QCD perturbation theory and contain an additional scale, $\mu_{\rm F}^2$. There are, in principle, two possibilities how to proceed any further. One option is provided by setting $\mu_{\rm F}^2 \simeq Q^2$ and then face the problem of analytization of terms like $[\alpha_s(Q^2)/\alpha_s(\mu_0^2)]^\eta$, where $\eta = \gamma_n^{(0)}/(2b_0)$ is a fractional number, as discussed in [36]. Another possibility is to fix the factorization scale $\mu_{\rm F}^2$ at some value and then to redefine the original Shirkov-Solovtsov analytization procedure in order to take the dispersive image of the coupling (or of its powers) together with these logarithmic terms. This second route is followed in the present work. It is important to note that the KS analytization procedure reduces in LO of fixed-order perturbation theory to the *maximal* one, as shown in [32], provided evolution effects of the pion distribution amplitudes are ignored.

Applying now this generalized analytization concept, we get

$$[Q^2 T_{\rm H}(x, y, Q^2; \mu_{\rm F}^2, \lambda_{\rm R} Q^2)]_{\rm KS}^{\rm an} = \mathcal{A}_1^{(2)}(\lambda_{\rm R} Q^2) t_{\rm H}^{(0)}(x, y) + \frac{\mathcal{A}_2^{(2)}(\lambda_{\rm R} Q^2)}{4\pi} (b_0 t_{\rm H}^{(1,\beta)}(x, y; \lambda_{\rm R}) + t_{\rm H}^{(\rm FG)}(x, y)) + \left[\frac{(\alpha_s^{(2)}(\lambda_{\rm R} Q^2))^2}{4\pi} C_{\rm F} t_{\rm H}^{(0)}(x, y)(6 + 2\ln(\bar{x}\bar{y})) \times \ln\frac{Q^2}{\mu_{\rm F}^2}\right]_{\rm KS}^{\rm an}. \tag{3.11}$$

In order to have the same scale argument in the logarithmic term as in the running coupling, we substitute $\ln(Q^2/\mu_{\rm F}^2) = \ln(\lambda_{\rm R} Q^2/\Lambda^2) - \ln(\lambda_{\rm R}\mu_{\rm F}^2/\Lambda^2)$ to obtain

$$[Q^2 T_{\rm H}(x, y, Q^2; \mu_{\rm F}^2, \lambda_{\rm R} Q^2)]_{\rm KS}^{\rm an} = \mathcal{A}_1^{(2)}(\lambda_{\rm R} Q^2) t_{\rm H}^{(0)}(x, y) + \frac{\mathcal{A}_2^{(2)}(\lambda_{\rm R} Q^2)}{4\pi} \times \left[b_0 t_{\rm H}^{(1,\beta)}(x, y; \lambda_{\rm R}) + t_{\rm H}^{(\rm FG)}(x, y) - C_{\rm F} t_{\rm H}^{(0)}(x, y)(6 + 2\ln(\bar{x}\bar{y}))\ln\frac{\lambda_{\rm R}\mu_{\rm F}^2}{\Lambda^2}\right] + \left[\frac{(\alpha_s^{(2)}(\lambda_{\rm R} Q^2))^2}{4\pi} C_{\rm F} t_{\rm H}^{(0)}(x, y)(6 + 2\ln(\bar{x}\bar{y}))\ln\frac{\lambda_{\rm R} Q^2}{\Lambda^2}\right]_{\rm KS}^{\rm an}. \tag{3.12}$$

Finally, we arrive at

[3] One should not worry about the factor $1/Q^2$ because under analytization it reproduces itself, i.e., $[[f(Q^2)]^{\rm an}/Q^2]^{\rm an} = [f(Q^2)]^{\rm an}/Q^2$.

$$
\begin{aligned}
&[Q^2 T_{\mathrm{H}}(x, y, Q^2; \mu_{\mathrm{F}}^2, \lambda_{\mathrm{R}} Q^2)]_{\mathrm{KS}}^{\mathrm{an}} \\
&= \mathcal{A}_1^{(2)}(\lambda_{\mathrm{R}} Q^2) t_{\mathrm{H}}^{(0)}(x, y) + \frac{\mathcal{A}_2^{(2)}(\lambda_{\mathrm{R}} Q^2)}{4\pi} \\
&\quad \times [b_0 t_{\mathrm{H}}^{(1,\beta)}(x, y; \lambda_{\mathrm{R}}) + t_{\mathrm{H}}^{(\mathrm{FG})}(x, y) \\
&\quad + C_{\mathrm{F}} t_{\mathrm{H},2}^{(1,\mathrm{F})}\left(x, y; \frac{\mu_{\mathrm{F}}^2}{Q^2}\right)\Big] + \frac{\Delta_2^{(2)}(\lambda_{\mathrm{R}} Q^2)}{4\pi} \\
&\quad \times [C_{\mathrm{F}} t_{\mathrm{H}}^{(0)}(x, y)(6 + 2\ln(\bar{x}\bar{y}))], \qquad (3.13)
\end{aligned}
$$

where the deviation from Eq. (3.10) is encoded in the term

$$\Delta_2^{(2)}(Q^2) \equiv \mathcal{L}_2^{(2)}(Q^2) - \mathcal{A}_2^{(2)}(Q^2) \ln[Q^2/\Lambda^2] \qquad (3.14)$$

with

$$
\begin{aligned}
\mathcal{L}_2^{(2)}(Q^2) &\equiv \left[(\alpha_s^{(2)}(Q^2))^2 \ln\left(\frac{Q^2}{\Lambda^2}\right) \right]_{\mathrm{KS}}^{\mathrm{an}} \\
&= \frac{4\pi}{b_0} \left[\frac{(\alpha_s^{(2)}(Q^2))^2}{\alpha_s^{(1)}(Q^2)} \right]_{\mathrm{KS}}^{\mathrm{an}}. \qquad (3.15)
\end{aligned}
$$

It is important to distinguish between the two contributions in Eq. (3.14). The first amounts to the analytization of the product of the coupling with a logarithm, or equivalently of fractional powers of the coupling, as shown in [36]. The second bears an additional logarithmic dependence on the momentum scale Q^2 relative to the expression obtained with the *maximal* analytization procedure. The subscript KS in the last equation signifies that this expression should be analyticized according to the KS prescription. To obtain a clearer idea of its meaning and demonstrate its essence, the analytization is performed in three incremental steps. First, a simplified version of this expression is considered, which results by provisionally replacing the two-loop coupling in the numerator by its one-loop counterpart. Then, the ratio of the couplings after analytization reduces to [dash-dotted line in Fig. 1(a)]

$$\mathcal{L}_2^{(1)\mathrm{approx}}(Q^2) = \frac{4\pi}{b_0} \mathcal{A}_1^{(1)}(Q^2). \qquad (3.16)$$

Second, we discuss an analogous situation, in which the one-loop coupling in the denominator is (inconsistently) traded for its two-loop counterpart. In this case, the ratio of the couplings after analytization becomes [dashed line in Fig. 1(a)]

$$\mathcal{L}_2^{(2)\mathrm{approx}}(Q^2) = \frac{4\pi}{b_0} \mathcal{A}_1^{(2)}(Q^2). \qquad (3.17)$$

Finally, we provide the exact result for the KS analytization of expression (3.15) [solid line in Fig. 1(a)], with the derivation presented in Appendix C, while more general expressions are given in [36]:

$$\mathcal{L}_2^{(2)}(Q^2) = \frac{4\pi}{b_0} \left[\mathcal{A}_1^{(2)}(Q^2) + c_1 \frac{4\pi}{b_0} f_{\mathcal{L}}(Q^2) \right], \qquad (3.18)$$

where

$$
\begin{aligned}
f_{\mathcal{L}}(Q^2) = \sum_{n \geq 0} \left[\psi(2)\zeta(-n-1) - \frac{d\zeta(-n-1)}{dn} \right] \\
\times \frac{[-\ln(Q^2/\Lambda^2)]^n}{\Gamma(n+1)} \qquad (3.19)
\end{aligned}
$$

and $\zeta(z)$ is the Riemann zeta function. Equation (3.14) is illustrated in Fig. 1(b) for the different expressions of $\mathcal{L}_2(Q^2)$ given by Eqs. (3.16), (3.17), and (3.18) using the same line designations as in Fig. 1(a). Let us close this discussion by commenting that in the region where there are experimental data available [54,55] (i.e., well below 10 GeV^2), Eq. (3.14) is governed by $\mathcal{L}_2^{(2)}(Q^2)$, which entails a small enhancement of the hard-scattering amplitude for $Q^2 \leq 7.25$ GeV^2.

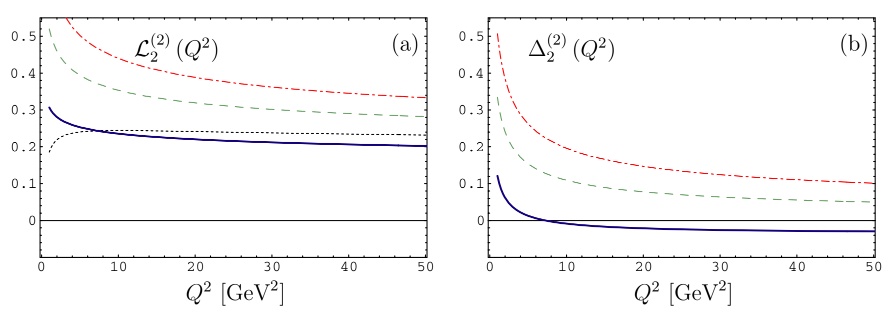

FIG. 1 (color online). (a) Results for the analyticized logarithmic term, $\mathcal{L}_2^{(2)}(Q^2)$, using three different analytization procedures: the one-loop approximate KS "analytization," $\mathcal{L}_2^{(1)\mathrm{approx}}(Q^2)$ (red dash-dotted line), the two-loop approximate KS "analytization," $\mathcal{L}_2^{(2)\mathrm{approx}}(Q^2)$ (green dashed line), and the exact two-loop BMKS analytization $\mathcal{L}_2^{(2)}(Q^2)$ (blue solid line). For comparison, we also show here the corresponding *maximal* analytization curve (dotted line). (b): Results are shown for the corresponding analyticized contributions $\Delta_2^{(2)}(Q^2)$, using the same three analytization procedures for $\mathcal{L}_2^{(2)}(Q^2)$ as in panel (a).

IV. FACTORIZED PION FORM FACTOR AT NLO—STANDARD AND ANALYTICIZED

The calculation of the factorized pion form factor proceeds in terms of Eq. (2.1) and involves the convolution of expression (3.10) for the *maximal* analytization case, or expression (3.13) for the KS analytization case with the pion DA for which we employ in both cases the BMS parametrization [41], as discussed in Sec. II. On that basis, we can obtain the scaled, factorized part of the pion form factor, $Q^2 F_\pi^{\rm Fact}(Q^2; \mu_{\rm R}^2 = \lambda_{\rm R} Q^2)$, using Eq. (2.8) and the following set of substitutions[4]:

$$t_{\rm H}^{(0)}(x, y) \rightarrow 8\pi f_\pi^2 (1 + a_2 + a_4)^2; \qquad (4.1)$$

$$-t_{\rm H}^{(0)}(x, y) \ln \bar{x}\,\bar{y} \rightarrow 8\pi f_\pi^2 (1 + a_2 + a_4)[3 + (43/6)a_2 + (136/15)a_4]; \qquad (4.2)$$

$$t_{\rm H}^{(\rm FG)}(x, y) \rightarrow 8\pi f_\pi^2 [-15.67 - a_2(21.52 - 6.22a_2) - a_4(7.37 - 37.40a_2 - 33.61a_4)]. \qquad (4.3)$$

Notice that evolving the BMS pion DA from the initial scale μ_0^2 to the scale $\mu_{\rm F}^2$ at the NLO level will generate higher Gegenbauer harmonics of the form $x\bar{x}C_{2n}^{3/2}(2x - 1)$ with $n \geq 3$. However, we have shown in [35] (see also [56]) that for the calculation of the pion form factor it is actually sufficient to restrict ourselves to the LO evolution and neglect NLO evolution effects. Hence, for our purposes in the present analysis, we set

$$a_{2n}(\mu_{\rm F}^2) = a_{2n}(\mu_0^2)\left[\frac{\alpha_s(\mu_{\rm F}^2)}{\alpha_s(\mu_0^2)}\right]^{\gamma_n^{(0)}/(2b_0)}. \qquad (4.4)$$

The lowest-order anomalous dimensions can be represented in closed form by

$$\gamma_n^{(0)} = 2C_{\rm F}\left[4S_1(n + 1) - 3 - \frac{2}{(n + 1)(n + 2)}\right] \qquad (4.5)$$

with $S_1(n + 1) = \sum_{i=1}^{n+1} 1/i = \psi(n + 2) - \psi(1)$, while the function $\psi(z)$ is defined as $\psi(z) = d\ln\Gamma(z)/dz$.

Following the master plan for "analytization," exposed in the previous section, we obtain the following expressions for the factorized pion form factor:

(i) *Naive* analytization [30,31,35]:

$$[F_\pi^{\rm Fact}(Q^2; \lambda_{\rm R} Q^2)]_{\rm NaivAn} = \mathcal{A}_1^{(2)}(\lambda_{\rm R} Q^2)\mathcal{F}_\pi^{\rm LO}(Q^2) + \frac{1}{\pi}[\mathcal{A}_1^{(2)}(\lambda_{\rm R} Q^2)]^2 \times \mathcal{F}_\pi^{\rm NLO}(Q^2, \mu_{\rm F}^2; \lambda_{\rm R}). \qquad (4.6)$$

(ii) *Maximal* analytization [35]:

$$[F_\pi^{\rm Fact}(Q^2; \lambda_{\rm R} Q^2)]_{\rm MaxAn} = \mathcal{A}_1^{(2)}(\lambda_{\rm R} Q^2)\mathcal{F}_\pi^{\rm LO}(Q^2) + \frac{1}{\pi}\mathcal{A}_2^{(2)}(\lambda_{\rm R} Q^2) \times \mathcal{F}_\pi^{\rm NLO}(Q^2, \mu_{\rm F}^2; \lambda_{\rm R}). \qquad (4.7)$$

(iii) KS *amplitude* analytization (this work)—cf. Eqs. (3.13), (3.14), and (3.15):

$$[F_\pi^{\rm Fact}(Q^2; \lambda_{\rm R} Q^2)]_{\rm KS} = \mathcal{A}_1^{(2)}(\lambda_{\rm R} Q^2)\mathcal{F}_\pi^{\rm LO}(Q^2) + \frac{1}{\pi}\mathcal{A}_2^{(2)}(\lambda_{\rm R} Q^2) \times \mathcal{F}_\pi^{\rm NLO}(Q^2, \mu_{\rm F}^2; \lambda_{\rm R}) + \frac{\Delta_2^{(2)}(\lambda_{\rm R} Q^2)}{\pi}\Delta_{\rm F}\mathcal{F}_\pi^{\rm NLO}(Q^2). \qquad (4.8)$$

Here we use the following notations:

$$\mathcal{F}_\pi^{\rm LO}(Q^2) = \frac{8\pi f_\pi^2}{Q^2}(1 + a_2 + a_4)^2; \qquad (4.9)$$

$$\mathcal{F}_\pi^{\rm NLO}(Q^2, \mu_{\rm F}^2; \lambda_{\rm R}) = \frac{2\pi f_\pi^2}{Q^2}[b_0(1 + a_2 + a_4)^2(\ln\lambda_{\rm R} - \ln\lambda_{\rm BLM}(a_2, a_4)) - 15.67 - a_2(21.52 - 6.22a_2) - a_4(7.37 - 37.40a_2 - 33.61a_4)] + \Delta_{\rm F}\mathcal{F}_\pi^{\rm NLO}(Q^2)\ln\frac{Q^2}{\mu_{\rm F}^2} \qquad (4.10)$$

and we explicitly display the contribution due to $t_{\rm H,2}^{(1,\rm F)}(x, y; \mu_{\rm F}^2/Q^2)$, see Eq. (2.7b):

$$\Delta_{\rm F}\mathcal{F}_\pi^{\rm NLO}(Q^2) = -\frac{2\pi f_\pi^2}{Q^2}C_{\rm F}(1 + a_2 + a_4)[(25/3)a_2 + (182/15)a_4]. \qquad (4.11)$$

In order to make our formulas more compact, we implement the BLM scale:

$$\lambda_{\rm BLM}(a_2, a_4) = \exp\left[-\frac{5}{3} - \frac{3 + (43/6)a_2 + (136/15)a_4}{1 + a_2 + a_4}\right]. \qquad (4.12)$$

The analytization augmented perturbation theory works very well. This is illustrated by the results in Figs. 2–4. The first of these figures compares the specific issues of the KS

[4]Here, we write for the sake of brevity $a_2 = a_2^{\rm BMS}(\mu_{\rm F}^2)$ and $a_4 = a_4^{\rm BMS}(\mu_{\rm F}^2)$ and use the values given in Eq. (2.11).

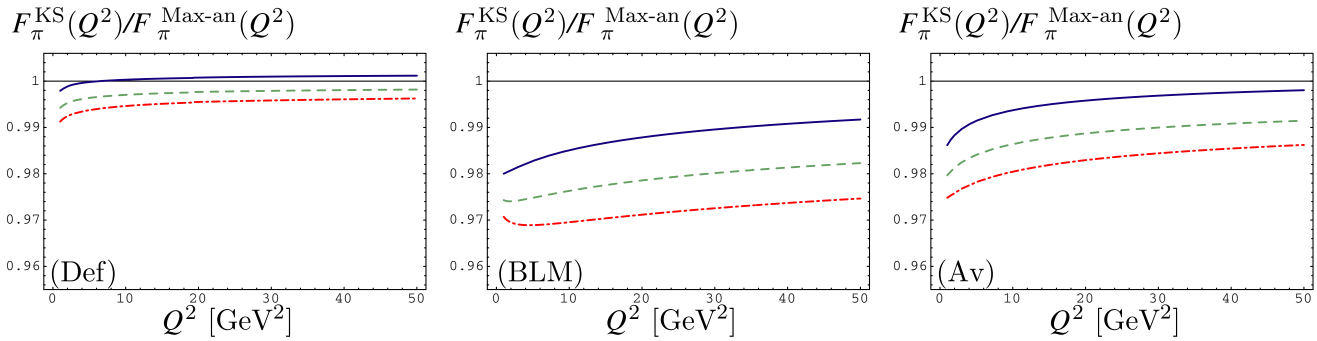

FIG. 2 (color online). Results for the ratio of the factorized pion form factors, using two different analytization procedures: KS analytization and "maximal analytization," $F_\pi^{\rm KS}(Q^2)/F_\pi^{\rm Max\text{-}an}(Q^2)$. The designations are: red dash-dotted line—one-loop approximation of the KS logarithmic term ($\mathcal{L}_2^{(1)\rm approx}(Q^2)$); green dashed line—two-loop approximation ($\mathcal{L}_2^{(2)\rm approx}(Q^2)$); blue solid line—exact two-loop KS analytization ($\mathcal{L}_2^{(2)}(Q^2)$). Left panel: default scale setting ($\lambda = 1$); middle panel: BLM scale setting; right panel: α_V scheme. The factorization scale $\mu_{\rm F}^2$ is set equal to 5.76 GeV^2 [57].

analytization procedure relative to those of the *maximal* one for the ratio of the corresponding factorized form factors. A few words are in order here. One sees that using the default $\overline{\rm MS}$ scheme, the KS analytization procedure yields a result almost coincident with that provided by the *maximal* one. On the other hand, in the BLM scheme and also in the α_V scheme, the KS prediction is smaller by a few percent. Moreover, one observes by comparison with Fig. 1(a), right panel in Ref. [35] that the BLM prediction, which in the *maximal* procedure was the largest one, becomes in the case of the KS prescription comparable with the prediction of the default scheme. As a result, the inherent theoretical uncertainties due to the involved perturbative parameters, defining a renormalization scheme and scale setting, are further reduced. A second important feature of the KS procedure is that the dependence of $F_\pi^{\rm Fact}(Q^2)$ on the factorization scale is almost diminished, as indicated in Fig. 3. Indeed, varying the factorization scale from 1 to 10 GeV^2, the form factor changes by a mere 1.5%. Even setting the factorization scale to the theoretical value of 50 GeV^2, the induced variation in the form-factor magnitude reaches just the level of about 2.5%. In the case of the *maximal* analytization procedure, the dependence on the factorization scale is also a mild one, but the corresponding variation is, in round terms, 2 times larger.

The fourth figure demonstrates the impact of analytization on the factorized pion's electromagnetic form factor, using various analytization prescriptions. The dashed line denotes the prediction obtained with standard QCD perturbation theory in the $\overline{\rm MS}$ scheme and applying the default scale setting $\mu_{\rm R}^2 = Q^2$. The *naive* analytization prediction is represented by the dash-dotted line and the analogous one for the *maximal* analytization by the solid line below it. The result of the calculation according to the KS analytization practically coincides with that of the *maximal* one. This behavior is also reflected in Fig. 2, where we see that the differences among the three analytization procedures are of the order of a few percent in the whole Q^2 range considered.

Note that as regards the whole pion form factor, i.e., taking into account also the soft part, the differences would be further reduced. For full details the reader is referred to [35].

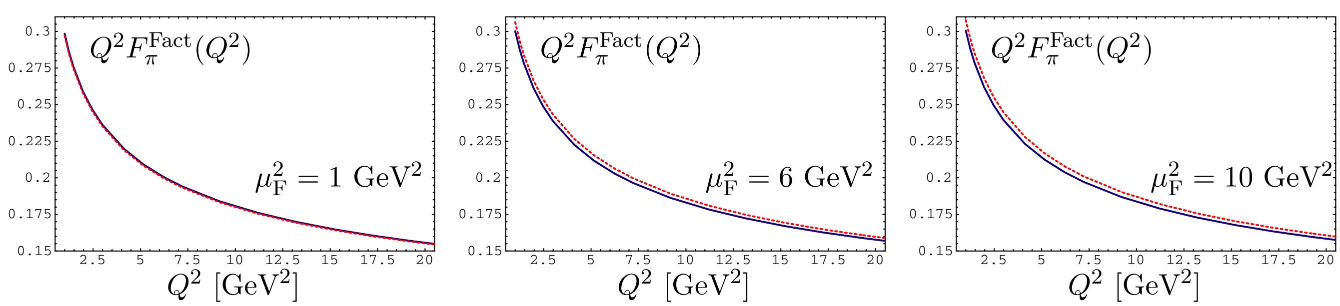

FIG. 3 (color online). Results for the factorized pion form factors, using two different analytization procedures: KS analytization (blue solid line) and "maximal analytization" (red dotted line) for different values of the factorization scale: in the left panel $\mu_{\rm F}^2 =$ 1 GeV^2, in the middle one—$\mu_{\rm F}^2 = 1$ GeV^2, and in the right one—$\mu_{\rm F}^2 = 10$ GeV^2. For all panels we show results for the BLM scale setting.

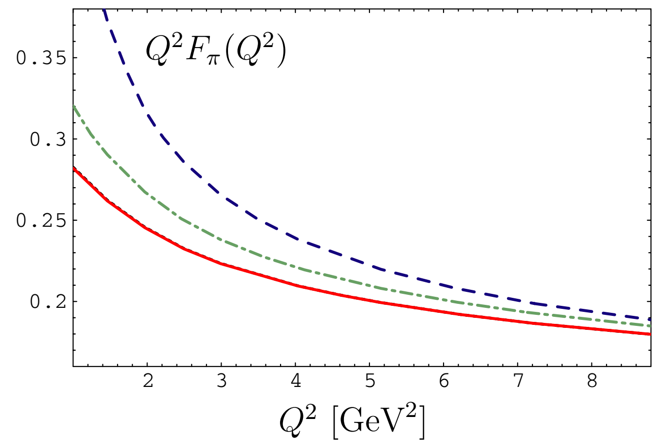

FIG. 4 (color online). Results for the factorized pion form factor, scaled with Q^2, and assuming the default scale setting ($\mu_R^2 = Q^2$) in standard perturbation theory and APT. The latter is implemented in terms of two different analytization procedures: *naive* analytization and *maximal* "analytization." The designations are: blue dashed line—standard perturbation theory; green dash-dotted line—*naive* APT; red solid line—*maximal* APT. The prediction obtained with the KS analytization is too close to that found with the *maximal* one to differentiate these curves graphically. The factorization scale μ_F^2 is set equal to 5.76 GeV^2.

V. SUMMARY AND CONCLUSIONS

We have discussed different analytization procedures to ensure the analyticity of the factorized electromagnetic pion form factor at NLO of QCD perturbation theory. The main features and relative merits of each analytization concept following from the presented analysis are the following:

(i) The *naive* "analytization [30,31] retains the power-series expansion of perturbative QCD, but replaces $(\alpha_s^{(n)}(Q^2))^m$ by $(\mathcal{A}_1^{(n)}(Q^2))^m$. As it was shown in [30,31], this reduces the value of the NLO correction, though the sensitivity to the renormalization scheme adopted and the renormalization-scale setting chosen is still substantial, resulting into a rather strong variation of the form-factor predictions [35]. Moreover, this procedure does not respect nonlinear relations of the coupling because these correspond to different dispersive images.

(ii) The *maximal* analytization [35] trades the power-series expansion for a functional nonpower-series expansion in terms of $\mathcal{A}_m^{(n)}(Q^2)$ [11,16,17], minimizing the variation of the form-factor predictions owing to the renormalization scheme and scale setting. It is, however, insufficient to cure logarithms of the momentum scale multiplying the running coupling. Such terms modify the spectral density, i.e., the discontinuity across the cut along the negative real axis and have therefore to be taken into account.

(iii) Applying the analytization procedure at the level of the partonic amplitude itself [32,33], bears all advantages of the *maximal* analytization plus a further reduced dependence on the perturbative scales—especially the dependence on the factorization scale. This has been verified by explicit calculation. We have employed the $\overline{\rm MS}$ scheme with various scale settings and also the α_V scheme. In addition, we have varied the factorization scale in the range 1–10 GeV^2. While the predictions for the factorized pion form factor, calculated with the *maximal* procedure, were affected by this variation on the level of 3%, their counterparts, derived with the KS prescription, were influenced by less than 1%. Though the KS method does not really "gain up" relative to the *maximal* analytization procedure with respect to the factorized pion form factor, as one observes from Fig. 4, it is able to further improve the perturbative treatment because it extends the notion of analyticity to noninteger powers of the strong running coupling—FAPT. Such powers become relevant when one has to calculate the analytic image of powers of the strong coupling in combination with logarithms, the latter first appearing at NLO of fixed-order perturbation theory, or in terms of evolution factors [36]. Hence, the KS analytization requirement treats all logarithms that have a nonzero spectral density, and hence modify the discontinuity across the cut along the negative real axis, on the same footing and irrespective of their source being it the running coupling (and its powers), or logarithms entailed by ERBL or DGLAP evolution.

In conclusion, the KS analytization enables the variation of the factorization scale and the choice of various renormalization schemes and scale settings, including the BLM one, with undiminished quality of the theoretical predictions from scheme (scale) to scheme (scale), virtually eliminating the dependence on such parameters and upgrading the $\overline{\rm MS}$ scheme to an optimized factorization and renormalization scheme. From a broader perspective one may interpret these findings as indicating that the analyticity of the partonic three-point function is as important and fundamental as the underlying symmetries of the theory and should be preserved together with them in the maximal possible way.

ACKNOWLEDGMENTS

We wish to thank Sergey Mikhailov for valuable discussions and comments. Two of us (A. P. B. and A. I. K.) are indebted to Professor Klaus Goeke for the warm hospitality at Bochum University, where the major part of this investigation was carried out. This work was supported in part by the Deutsche Forschungsgemeinschaft, the Verbundforschung des Bundesministeriums für Bildung und Forschung, the Heisenberg–Landau Programme (Grant 2005), and the Russian Foundation for Fundamental Research (Grants No. 03-02-16816, No. 03-02-04022 and No. 05-01-00992).

APPENDIX A: QCD β FUNCTION AT NLO

The first coefficients of the β function are

$$b_0 = \frac{11}{3} C_{\rm A} - \frac{4}{3} T_{\rm R} N_f, \qquad b_1 = \frac{34}{3} C_{\rm A}^2 - \left(4C_{\rm F} + \frac{20}{3} C_{\rm A}\right) T_{\rm R} N_f. \tag{A1}$$

Here, $T_{\rm R} = 1/2$ and N_f denotes the number of flavors, whereas the expansion of the β function in the NLO approximation is given by

$$\beta(\alpha_s(\mu^2)) = -\alpha_s(\mu^2)\left[b_0\left(\frac{\alpha_s(\mu^2)}{4\pi}\right) + b_1\left(\frac{\alpha_s(\mu^2)}{4\pi}\right)^2\right]. \tag{A2}$$

APPENDIX B: NLO CORRECTION TO THE PION FORM FACTOR

Here we present the detailed expressions for the color decomposition of the NLO correction to the hard amplitude $T_{\rm H}$, which describe the factorized part of the pion form factor [35,39] (see Eqs. (2.5), (2.6a)–(2.6c), (2.7a), and (2.7b):

$$t_{\rm H,1}^{(1,{\rm F})}(x,y) = \frac{N_{\rm T}}{\bar{x}\,\bar{y}}\left[-\frac{28}{3} + \left(6 - \frac{1}{x}\right)\ln\bar{x} + \left(6 - \frac{1}{y}\right)\ln\bar{y} + \ln^2(\bar{x}\,\bar{y})\right]; \tag{B1}$$

$$t_{\rm H}^{(1,{\rm G})}(x,y) = \frac{2N_{\rm T}}{\bar{x}\,\bar{y}}\left[-\frac{10}{3} + \ln\left(\frac{\bar{x}}{x}\right)\ln\left(\frac{y}{\bar{y}}\right) - 4\left(\frac{\ln\bar{x}}{x} + \frac{\ln\bar{y}}{y}\right) - \tilde{H}(x,y) - R(x,y)\right]. \tag{B2}$$

The functions $\tilde{H}(x,y)$ and $R(x,y)$ are defined by

$$\tilde{H}(x,y) = \left[\mathbf{Li}_2\left(\frac{\bar{y}}{x}\right) + \mathbf{Li}_2\left(\frac{\bar{x}}{y}\right) + \mathbf{Li}_2\left(\frac{xy}{\bar{x}\,\bar{y}}\right) - \mathbf{Li}_2\left(\frac{x}{\bar{y}}\right) - \mathbf{Li}_2\left(\frac{y}{\bar{x}}\right) - \mathbf{Li}_2\left(\frac{\bar{x}\,\bar{y}}{xy}\right)\right] \tag{B3}$$

and

$$R(x,y) = \frac{1}{(x-y)^2}\Big[(2xy - x - y)(\ln x + \ln y) - (y\bar{y}^2 + x\bar{x}^2)(1-x-y)\tilde{H}(x,\bar{y}) - 2(xy^2 + y^2 - 5xy + y + 2x^2)\frac{\ln\bar{y}}{y} - 2(yx^2 + x^2 - 5xy + x + 2y^2)\frac{\ln\bar{x}}{x}\Big]. \tag{B4}$$

APPENDIX C: ANALYTIZATION OF POWERS OF THE COUPLING MULTIPLIED BY LOGARITHMS

We present here the derivation of $\mathcal{L}_2^{(2)}(Q^2)$, done in collaboration with Mikhailov. To this end, let us first introduce

$$a_s(Q^2) \equiv \frac{b_0}{4\pi}\alpha_s(Q^2). \tag{C1}$$

For this quantity we can write a renormalization group solution in the form

$$[a_s^{(2)}(Q^2)]^2 \ln\left(\frac{Q^2}{\Lambda^2}\right) = a_s^{(2)}(Q^2) + [a_s^{(2)}(Q^2)]^2 c_1 \ln\left[\frac{a_s^{(2)}(Q^2)}{1 + c_1 a_s^{(2)}(Q^2)}\right]. \tag{C2}$$

Expanding the expression $\ln[1 + c_1 a_s^{(2)}(Q^2)]$ and retaining terms up to order a_s^2, we find

$$[a_s^{(2)}(Q^2)]^2 \ln\left(\frac{Q^2}{\Lambda^2}\right) = a_s^{(2)}(Q^2) + [a_s^{(2)}(Q^2)]^2 c_1 \ln[a_s^{(2)}(Q^2)]. \tag{C3}$$

To get rid of the logarithm, we use the following trick

$$[a_s^{(2)}(Q^2)]^2 \ln\left(\frac{Q^2}{\Lambda^2}\right) = a_s^{(2)}(Q^2) + c_1 \frac{d}{d\varepsilon}[a_s^{(2)}(Q^2)]^{2+\varepsilon}|_{\varepsilon=0} \tag{C4}$$

and return to the original coupling to obtain

$$[\alpha_s^{(2)}(Q^2)]^2 \ln\left(\frac{Q^2}{\Lambda^2}\right) = \frac{4\pi}{b_0}\alpha_s^{(2)}(Q^2) + c_1 \frac{4\pi}{b_0}\frac{d}{d\varepsilon} \times [\alpha_s^{(2)}(Q^2)]^{2+\varepsilon}|_{\varepsilon=0}. \tag{C5}$$

Now we can proceed with the "analytization" of the term $[\alpha_s^{(2)}(Q^2)]^2 \ln(Q^2)$, giving rise to analytic expressions for noninteger powers of the coupling, i.e.,

$$\left\{\left[\alpha_s^{(2)}(Q^2)\right]^2 \ln\left(\frac{Q^2}{\Lambda^2}\right)\right\}_{\text{an}} = \frac{4\pi}{b_0}\mathcal{A}_1^{(2)}(Q^2) + c_1\left[\frac{d}{d\varepsilon}\mathcal{A}_{2+\varepsilon}^{(2)}(Q^2)\right]_{\varepsilon=0}. \quad \text{(C6)}$$

Using the representation [36]

$$\left(\frac{b_0}{4\pi}\right)^2 \mathcal{A}_\nu^{(2)}(Q^2) = \frac{-1}{\Gamma(\nu)}\sum_{n\geq 0}\zeta(1-\nu-n)\frac{[-\ln(Q^2/\Lambda^2)]^n}{\Gamma(n+1)} \quad \text{(C7)}$$

and performing the differentiation, we finally obtain

$$\left\{[\alpha_s^{(2)}(Q^2)]^2 \ln\left(\frac{Q^2}{\Lambda^2}\right)\right\}_{\text{an}} = \frac{4\pi}{b_0}\left[\mathcal{A}_1^{(2)}(Q^2) + c_1\frac{4\pi}{b_0}f_{\mathcal{L}}(Q^2)\right], \quad \text{(C8)}$$

with $f_{\mathcal{L}}(Q^2)$ being defined in Eq. (3.19).

[1] J. M. Cornwall, Phys. Rev. D **26**, 1453 (1982).
[2] G. Parisi and R. Petronzio, Nucl. Phys. **B154**, 427 (1979).
[3] C. R. Ji, A. F. Sill, and R. M. Lombard-Nelsen, Phys. Rev. D **36**, 165 (1987).
[4] N. G. Stefanis, Phys. Rev. D **40**, 2305 (1989); N. G. Stefanis, Phys. Rev. D **44**, 1616(E) (1991).
[5] C. R. Ji and F. Amiri, Phys. Rev. D **42**, 3764 (1990).
[6] N. G. Stefanis and M. Bergmann, Phys. Lett. B **304**, 24 (1993).
[7] A. C. Mattingly and P. M. Stevenson, Phys. Rev. D **49**, 437 (1994).
[8] S. J. Brodsky, C. R. Ji, A. Pang, and D. G. Robertson, Phys. Rev. D **57**, 245 (1998).
[9] D. Müller, Phys. Rev. D **59**, 116003 (1999).
[10] N. G. Stefanis, Eur. Phys. J. direct C **7**, 1 (1999).
[11] D. V. Shirkov and I. L. Solovtsov, Phys. Rev. Lett. **79**, 1209 (1997).
[12] D. V. Shirkov, Theor. Math. Phys. **119**, 438 (1999) [Teor. Mat. Fiz. **119**, 55 (1999)].
[13] I. L. Solovtsov and D. V. Shirkov, Theor. Math. Phys. **120**, 1220 (1999) [Teor. Mat. Fiz. **120**, 482 (1999)].
[14] D. V. Shirkov, hep-ph/0003242; hep-ph/0009106; hep-ph/0408272.
[15] I. L. Solovtsov and D. V. Shirkov, Phys. Lett. B **442**, 344 (1998).
[16] D. V. Shirkov, Theor. Math. Phys. **127**, 409 (2001); Eur. Phys. J. C **22**, 331 (2001).
[17] D. V. Shirkov and I. L. Solovtsov, Phys. Part. Nucl. **32S1**, 48 (2001).
[18] D. S. Kourashev and B. A. Magradze, hep-ph/0104142 (unpublished); Theor. Math. Phys. **135**, 531 (2003) [Teor. Mat. Fiz. **135**, 95 (2003)].
[19] B. A. Magradze, Int. J. Mod. Phys. A **15**, 2715 (2000); hep-ph/0010070; hep-ph/0305020.
[20] S. J. Brodsky, S. Menke, C. Merino, and J. Rathsman, Phys. Rev. D **67**, 055008 (2003).
[21] A. I. Alekseev, hep-ph/0503242.
[22] A. V. Radyushkin, JINR Rapid Commun. **78**, 96 (1996).
[23] N. V. Krasnikov and A. A. Pivovarov, Phys. Lett. B **116**, 168 (1982).
[24] M. Beneke and V. M. Braun, Phys. Lett. B **348**, 513 (1995).
[25] P. Ball, M. Beneke, and V. M. Braun, Nucl. Phys. **B452**, 563 (1995).
[26] K. A. Milton and I. L. Solovtsov, Phys. Rev. D **55**, 5295 (1997); K. A. Milton, I. L. Solovtsov, and O. P. Solovtsova, Phys. Lett. B **415**, 104 (1997).
[27] A. P. Bakulev, A. V. Radyushkin, and N. G. Stefanis, Phys. Rev. D **62**, 113001 (2000).
[28] A. V. Nesterenko, Int. J. Mod. Phys. A **18**, 5475 (2003); Int. J. Mod. Phys. A **18**, 5475 (2003).
[29] A. V. Nesterenko and J. Papavassiliou, Phys. Rev. D **71**, 016009 (2005); hep-ph/0410072; A. C. Aguilar, A. V. Nesterenko, and J. Papavassiliou, J. Phys. G **31**, 997 (2005).
[30] N. G. Stefanis, W. Schroers, and H. C. Kim, Phys. Lett. B **449**, 299 (1999).
[31] N. G. Stefanis, W. Schroers, and H. C. Kim, Eur. Phys. J. C **18**, 137 (2000).
[32] A. I. Karanikas and N. G. Stefanis, Phys. Lett. B **504**, 225 (2001).
[33] N. G. Stefanis, Lect. Notes Phys. **616**, 153 (2003); hep-ph/0410245 [Nucl. Phys. Proc. Suppl. (to be published)].
[34] S. J. Brodsky and H. J. Lu, Phys. Rev. D **51**, 3652 (1995).
[35] A. P. Bakulev, K. Passek-Kumerički, W. Schroers, and N. G. Stefanis, Phys. Rev. D **70**, 033014 (2004); A. P. Bakulev, K. Passek-Kumerički, W. Schroers, and N. G. Stefanis, Phys. Rev. D **70**, 079906(E) (2004); N. G. Stefanis, A. P. Bakulev, S. V. Mikhailov, K. Passek-Kumerički, and W. Schroers, hep-ph/0409176 (to be published).
[36] A. P. Bakulev, S. V. Mikhailov, and N. G. Stefanis, hep-ph/0506311 [Phys. Rev. D (to be published)].
[37] A. V. Efremov and A. V. Radyushkin, Phys. Lett. B **94**, 245 (1980); Theor. Math. Phys. **42**, 97 (1980).
[38] G. P. Lepage and S. J. Brodsky, Phys. Rev. D **22**, 2157 (1980).
[39] B. Melić, B. Nižić, and K. Passek, Phys. Rev. D **60**, 074004 (1999); B. Melić, B. Nižić, and K. Passek, Phys. Rev. D **65**, 053020 (2002).
[40] S. J. Brodsky, G. P. Lepage, and P. B. Mackenzie, Phys. Rev. D **28**, 228 (1983).
[41] A. P. Bakulev, S. V. Mikhailov, and N. G. Stefanis, Phys. Lett. B **508**, 279 (2001); A. P. Bakulev, S. V. Mikhailov, and N. G. Stefanis, Phys. Lett. B **590**, 309(E) (2004); in *Proceedings of the 36th Rencontres De Moriond On QCD And Hadronic Interactions, 17-24 Mar 2001, Les Arcs, France*, edited by J. T. T. Van (World Scientific, Singapore,

2002), p. 133.
[42] A. P. Bakulev, S. V. Mikhailov, and N. G. Stefanis, Phys. Rev. D **67**, 074012 (2003).
[43] A. P. Bakulev, S. V. Mikhailov, and N. G. Stefanis, Phys. Lett. B **578**, 91 (2004); Phys. Part. Nucl. **35**, 7 (2004).
[44] J. Gronberg *et al.* (CLEO Collaboration), Phys. Rev. D **57**, 33 (1998) .
[45] A. P. Bakulev, S. V. Mikhailov, and N. G. Stefanis, Ann. Phys. (Berlin) **13**, 629 (2004).
[46] H. .J. Behrend *et al.* (CELLO Collaboration), Z. Phys. C **49**, 401 (1991).
[47] Y. L. Dokshitzer, G. Marchesini, and B. R. Webber, Nucl. Phys. **B469**, 93 (1996).
[48] H. Contopanagos and G. Sterman, Nucl. Phys. **B419**, 77 (1994).
[49] S. Catani, M. L. Mangano, P. Nason, and L. Trentadue, Nucl. Phys. **B478**, 273 (1996).
[50] L. Magnea, Nucl. Phys. **B593**, 269 (2001).
[51] E. Gardi, Nucl. Phys. **B622**, 365 (2002).
[52] R. Alkofer and L. von Smekal, Phys. Rep. **353**, 281 (2001).
[53] M. Baldicchi and G. M. Prosperi, in *Proceedings of Wako 2003, Color Confinement and Hadrons in Quantum Chromodynamics, Wako, Japan, 2003* (World Scientific Publishing Company, Singapore, 2003), pp. 183–194; in *Quark Confinement and the Hadron Spectrum VI*, AIP Conf. Proc. No. 756 (AIP, New York, 2005), p. 152.
[54] J. Volmer *et al.* (Jefferson Lab F(pi) Collaboration), Phys. Rev. Lett. **86**, 1713 (2001); H. P. Blok, G. M. Huber, and D. J. Mack, nucl-ex/0208011.
[55] C. N. Brown *et al.*, Phys. Rev. D **8**, 92 (1973); C. J. Bebek *et al.*, Phys. Rev. D **13**, 25 (1976).
[56] A. P. Bakulev and N. G. Stefanis, Nucl. Phys. **B721**, 50 (2005).
[57] A. Schmedding and O. Yakovlev, Phys. Rev. D **62**, 116002 (2000).